Assessing the Catalytic Behavior of Platinum Group Metal-based Ultrathin Nanowires Using X-ray Absorption Spectroscopy

Nathaniel Hurley,[1] Scott C. McGuire,[1] and Stanislaus S. Wong[1,*]

Email: stanislaus.wong@stonybrook.edu

[1]Department of Chemistry, State University of New York at Stony Brook,

Stony Brook, NY 11794-3400

*To whom correspondence should be addressed.

Abstract:

Ultrathin metal-based nanowires have excelled as electrocatalysts in small-molecule reactions, such as the oxygen reduction reaction (ORR), the methanol oxidation reaction (MOR), and the ethanol oxidation reaction (EOR), and have consistently outperformed analogous Pt/C standards. As such, a detailed understanding of the structural and electronic properties of ultrathin nanowires is essential in terms of understanding structure-property correlations, which are crucial in the rational design of ever more sophisticated electrocatalysts. X-ray absorption spectroscopy (XAS) represents an important and promising characterization technique with which to acquire unique insights into the electronic structure and the local atomic structure of nanomaterials. Herein, we discuss tangible examples of how both *ex situ* and *in situ* XAS experiments have been recently applied to understanding the complex behavior of ultrathin nanowires used in electrocatalysis. Moreover, based on this precedence, we provide ideas about the future potential and direction of these ongoing efforts.

Keywords: platinum, X-ray absorption spectroscopy, catalysis, nanowires, fuel cells, alloys, and core-shell motifs

Introduction

Ultrathin nanowires (NWs) denote anisotropic one-dimensional (1D) motifs, characterized by average diameters of less than 10 nanometers. These ultrathin 1D structures possess many unique advantages, including (i) high surface areas due to their overall small dimensions and (ii) high-aspect ratios, along with the associated potential for (iii) long continuous crystalline planes and (iv) the ability to control structural defects along their longitudinal axis. These generally desirable attributes can give rise to advantageous catalytic enhancement due to superior reactivity, emanating from factors such as a mixture of surface strain effects coupled with large numbers of active sites. Despite the many benefits of ultrathin nanowires, some limitations remain with respect to their widespread applicability. These include (i) the intrinsic difficulty in terms of easily upscaling their synthesis to commercially relevant quantities as well as (ii) the fact that most ultrathin NWs reported in the literature tend to be composed of relatively rare and costly elements, such as Pt, Au, or Pd.

Moreover, varying the precise chemical composition and architecture of these ultrathin NWs represents additional means with which to not only promote performance but also reduce the overall quantity of scarce and expensive elemental components. For example, the creation of (a) ultrathin NW alloys enables the introduction of dopant elements that can synergistically give rise to a tailorable electronic structure. Additionally, (b) in the case of core-shell analogues of these materials, such as bimetallic, Pt-free alloy cores coated with a platinum monolayer shell, all loaded Pt atoms are available for catalysis, thereby reducing the total Pt content. In fact, the core metal-based substrate applies a compression strain and imparts a “ligand effect”, thereby lowering the Pt’s *d*-band energy and decreasing the affinity for passivating CO by weakening the Pt-CO bond, all of which can collectively tune the Pt for improved electrochemical activity.[1-2]

Ultrathin NWs have been synthesized using a variety of techniques, including but not limited to solution-based ligand-mediated growth, hydrothermal protocols, templating approaches, as well as ligand-directed, oriented attachment.[2] Conventionally, these materials have been studied using complementary characterization methods, including but not limited to X-ray photoelectron spectroscopy (XPS), X-ray diffraction (XRD), transmission electron microscopy (TEM), and energy dispersive spectroscopy (EDS), to yield key structural and chemical information about these motifs.

In this Perspective, we explore the equally significant but more recent impact that X-ray absorption spectroscopy (XAS) has yielded in terms of generating unique data streams and providing for unforeseen structure-property insights into the behavior of ultrathin NWs for electrocatalysis. Specifically, XAS uses X-rays to excite or ionize core electrons to a previously unoccupied electronic state (i.e., bound, quasi bound or continuum). Since the binding energy of core electrons is element specific, XAS is both element and core level specific.

X-ray absorption near-edge structure (XANES) denotes the region (i.e., ~50 eV above and below the ionization energy) within the XAS spectrum leading up to and at the absorption edge of an element. Specifically, K, L, and M-edges provide for a quantifiable estimate of the energy required to eject a 1*s;* 2*s* or 2*p;* and 3*s,* 3*p,* or 3*d* electron, respectively. As such, because XANES is inherently sensitive to charge states, it can provide information about the oxidation state of the elements being measured and the molecular structure, in addition to the electronic structure of materials. A comparison of the XANES white-line profile can often be used to identify the movement of electrons to and from the *d*-band, whose occupancy level is an indirect measure of catalyst stability, due to the fact that the position of the *d*-band energy is directly related to the binding energy of various types of poisoning species normally encountered during

electrocatalytic reactions. Features located at energies of ~50-1000 eV above the ionization energy encompass the extended X-ray absorption fine structure (EXAFS) region in which the observed oscillations are dependent upon the type, position, and number of neighboring atoms. Hence, EXAFS can be used to provide information about the local atomic structure, including coordination numbers (CN) and bond lengths. Moreover, the CN values of adjacent atomic pairs are often used to evaluate the extent of short-range order and/or ascertain the degree of compositional monodispersity within bimetallic alloyed samples.[3] The fundamentals of the XAS technique are more thoroughly discussed in the relevant prior literature.[4-6]

In practice, EXAFS can be used to differentiate among various different structurally nuanced configurations that can be found within a bimetallic system. These architectures include but are not limited to the formation of (a) a segregated structure, wherein there are particles consisting only of A atoms and particles comprised solely of B atoms, in which there is no alloying between the two metals; (b) a homogeneous structure in which there is a uniform distribution of atoms of different types within a chemically pure alloy; (c) a homophilic structure in which there is clustering of 'like' atoms, wherein there are A- or B-rich regions, but with mixing of the two different atom types; and finally, (d) a core-shell structure in which one atom segregates at the outer surface, whereas the other is localized within the inner center core. As such, EXAFS analysis is an innovative means with which to not only confirm alloy formation and degree of heterogeneity but also distinguish between distinctive alloying motifs (e.g., random versus ordered), especially in the presence of elemental segregation.[3, 7]

Given the profound capabilities of XAS, it is not surprising that it is beginning to be more widely used in the characterization of a whole host of nanomaterial systems, especially nanoparticles.[7-8] In this Perspective, as mentioned, we are interested in correlating the observed

catalytic performance with the structure of ultrathin NWs. Though the amount of literature on applying XAS to these narrow nanostructures is relatively limited, a few generalized and significant findings and trends seem to be relevant to the ensuing discussion. First, XAS can be used to not only distinguish and differentiate among distinctive chemical compositions, especially within different types of metal alloys, but also generate actionable data about the spatial localization of these constituent elements, notably within core-shell architectures. Second, whereas the majority of studies have thus far focused on *ex situ* analysis, the future resides in undertaking *in situ* studies in order to more fully probe the progression of the structure and chemistry of ultrathin NWs as a function of reaction time and evolving electrochemical reaction conditions in real time, which can more faithfully mimic those encountered by actual catalysts used in commercial applications. A corresponding *in situ* effort, which is beyond the scope of the current Perspective, has revolved around understanding the nature of the growth conditions that determine the nucleation and elongation of these NWs.[9]

Consequently, we explore these undercurrents of thought in the examination of not only ultrathin Pt, PtNi, and PtRh NWs but also their core shell analogues, such as PdAu@Pt, Au@Pd, and Au@Ag@Pd. It should be emphasized that XAS measurements, which reflect an 'averaged' snapshot, are rarely used to provide a definitive picture of the entire system at hand. Rather the story line is buttressed by key conclusions, emanating from complementary strands.

As examples, elemental mapping, images and line scans derived from high-resolution transmission electron microscopy (HRTEM) and accompanying EDS can corroborate the uniformity of morphology and composition of a sample.[10] X-ray or neutron-based pair distribution function (PDF) methods enable data collection of atomic distances, to affirm XAS conclusions.[8] XRD yields insights into the prevalence of contributions from different crystal

structures or species.[11] Data obtained by XAS can be further substantiated by analyzing subtle changes in either size distributions, morphology, packing arrangements, or crystallinity, as elucidated by small angle x-ray scattering (SAXS). Finally, measurements from either scanning tunneling microscopy (STM) or atomic force microscopy (AFM) can validate trends in local size and dilute elemental distributions.[9, 12-13] All of these techniques can be used to generate indispensable insights at the local level in a complementary manner to XAS data. Our own studies imply the need for a combined and collective consideration of not only XAS but also these other techniques in an effort to provide for an accurate representation of the local atomic structure of ultrathin NW motifs.

Discussion

We focus our discussion on the role of XAS in providing for insights into the catalytic behavior of ultrathin NWs. The vast majority of papers that have sought to use XAS to analyze ultrathin NWs have centered on Pt and its associated alloys. Due to its high activity, platinum is a commonly used catalyst for many different types of electrocatalytic reactions; for example, it represents one of the most active catalysts for ORR.[14-16] However, Pt is beset by a number of issues. Not only is Pt relatively rare and expensive but also, from an operational perspective, it suffers from poor stability and its surface can be easily poisoned by CO contamination.[17] Because of these serious concerns, Pt is often alloyed with other metals in order to enhance stability and durability and limit poisoning, so as to improve upon observed catalytic properties. Moreover, alloying also reduces the overall amount of costly, scarce Pt that is needed to be incorporated within functional catalysts. Not surprisingly, NWs of ultrathin Pt and their

associated alloys have been studied using XAS to provide for either *ex situ* or *in situ* data on their underlying viability as effective electrocatalysts.

***Ex Situ* XAS on ultrathin mono-metallic and alloy-based nanowires**

Jagged Pt ultrathin NWs (J-Pt NWs) with average diameters of 2.0 ± 0.2 nm were prepared using an "electrochemical de-alloying" process. This synthesis protocol involved the production of a $Pt_{15}Ni_{85}$ precursor alloy in which Ni atoms were leached away until only the desired Pt NWs remained.[18] The measured ORR activity for these systems was in the range of 11.5 mA/cm^2 at 0.90 V, which turned out to be not only ~7 times higher versus control wires (1.59 mA/cm^2) but also 32 times greater than a conventional Pt/C standard (0.35 mA/cm^2).

To account for this enhancement in catalytic performance, *ex situ* EXAFS measurements were obtained; these data showed that the coordination number for the Pt-Pt interactions was only 6-8, which was lower than the expected 8-9. The unexpected decrease in the CN was attributed to the roughened structure of the wires, because of the de-alloying process, which also had the corollary effect of increasing the number and density of active sites. In addition, a 1.8% decrease in the Pt-Pt bond length from 2.76 Å associated with the Pt control foil to 2.71 Å within the NWs was observed. Figure 1 A-D and Table 1 provide results not only on the structural nature of the NWs themselves but also on their associated EXAFS and CN measurements.

Moreover, these experimental results are similar to those obtained by a simulated radial distribution function for the J-Pt NWs, which proposed a bond length of ~2.70 Å, which is 2.5% shorter than the analogous distance predicted for Pt NW controls (2.76 Å). This measured decrease in the Pt-Pt bond length is suggestive of an increase in mechanical strain within the J-Pt NWs, as compared with either plain Pt NWs or bulk Pt foil, which would have resulted in a weakening of the binding energies of the adsorbed species, thereby leading to the observed

increase in activity. Overall, EXAFS analysis was crucial in explaining the large increase in ORR activity as emanating from a combination of shortening Pt-Pt bond lengths coupled with lower coordination numbers.[18]

To complement these studies, ultrathin Pt NWs, formed using a similar de-alloying process, were similarly reported as ORR catalysts.[19] Specifically, Pt NWs were generated by using $Pt(acac)_2$ as the metal source, oleylamine as the solvent, CTAB as the shape directing agent, and $Mo(CO)_6$ as the reducing agent. The corresponding PtNi NWs were formed using an impregnation method, in which the Pt NWs were sonicated in an aqueous solution with nickel nitrate, followed by annealing in an inert atmosphere. Finally, Pt NWs could be obtained again from PtNi by de-alloying in an oxygen saturated electrolyte solution, thereby yielding the desired **D-O_2-Pt NWs.** TEM measurements were consistent with the formation of NWs with average diameters measuring ~2 nm, while XRD, XPS, and inductively coupled plasma atomic emission spectrometry (ICP-AES) data collectively implied that all of the Ni atoms had been removed after the de-alloying process.

In effect, the D-O_2-Pt NWs achieved the highest specific and mass activities, as compared with both Pt NWs and Pt/C. To account for the observed enhancement in ORR activity, XAS data were acquired in order to probe the local atomic and electronic structure. To this end, the EXAFS fitting results implied that the D-O_2-Pt NWs were characterized by a smaller Pt-Pt CN value (7.59) as compared with that of Pt/C alone (9). This nominal decrease in the observed CN was attributed to de-alloying of the Ni atoms, which gave rise to a wide distribution of potential active site configurations (including concave and convex sites), all of which had the net collective effect of lowering the amount of Pt coordination. Table 1 highlights all of these measured CN values. As such, XAS analysis coupled with CO stripping

measurements suggested that the surfaces of these NWs were defect-rich, thereby leading to the apparent improvement in ORR activity.

PtRh ultrathin NWs have also been used as ORR catalysts. These were fabricated by a solution-based method in which $Pt(acac)_2$ and $Rh(acac)_3$ were used as precursors, didecyldimethylammonium bromide (DDAB) was utilized as a surfactant, $W(CO)_6$ was treated as a reducing agent, and oleylamine was employed as the solvent.[20] The resulting PtRh wires possessed widths and lengths of 1.3 ± 0.3 nm and 40.4 ± 15.1 nm, respectively, with an atomic ratio of Pt/Rh found to be ~7:1 using both XPS and ICP-AES. These motifs evinced an ORR specific activity of 1.63 mA/cm^{-2} at 0.9 V, which was 1.2x higher than that of pure Pt and 5.4x greater than that of commercial Pt/C. Moreover, these PtRh catalysts evinced significantly enhanced stability, losing only 9.2% of its total performance after 10,000 cycles as compared with 19.5% and 72.3% for standard Pt NWs and Pt/C, respectively.

To account for the improvement in ORR performance, analysis of the EXAFS spectra suggested that the Pt-Pt bond length had decreased by 0.7% as compared with the Pt foil control, an observation attributed not only to the thin diameter of the wires but also to the incorporation of the smaller radius Rh atoms within the resulting alloy. This bond length reduction likely induced a corresponding increase in strain, which improved upon ORR activity by weakening the adsorption energy of the surface bound hydroxyl groups by as much as 0.02 eV. The associated FT-EXAFS results and accompanying CN data are presented in Figure 1E and Table 1, respectively. Complementary density functional theory (DFT) and ICP-AES data indicated that the wires preferentially leached out Rh (as opposed to Pt) during the reaction process, implying that the presence of Rh was the likely cause for the increased NW stability, since it tended to degrade first as opposed to the surrounding Pt.[20]

***Ex Situ* XAS on ultrathin single-atom and core-shell nanowires**

An enhanced performance for hydrogen evolution reaction (HER), methanol oxidation reaction (MOR), and ethanol oxidation reaction (EOR) was correspondingly noted with **PtNi single atom alloys** (SAA), characterized by average diameters of ~2 nm and which had been created using the identical 'de-alloying' protocol.[21] Similarly with J-Pt NWs, EXAFS analysis was consistent with a 1.8% decrease in Pt-Pt bond lengths versus that of the Pt foil control. Study of the XANES white line for the PtNi SAAs demonstrated that Pt likely existed in the metallic state, matching closely to that of the Pt foil. The corresponding XANES features for the Ni *K*-edge closely resembled that of $Ni(OH)_2$, indicating the presence of Ni^{2+}. The EXAFS results at the Ni *K*-edge yielded a single peak at 1.6 Å, which can be attributed to the first shell Ni-O bond. However, there were no obvious peaks consistent with either Ni-Ni or Ni-O-Ni coordination, all of which implied that (i) there was no long-range coordination to other Ni atoms and that (ii) the Ni species likely existed as single, solitary atoms deposited at the surface. Table 2 summarizes the CN values and bond distances, derived from the EXAFS fitting. Furthermore, corroborating the EXAFS results, a series of HRTEM imaging coupled with electron energy loss spectroscopy (EELS) mapping experiments highlighted the expected distribution of Ni atoms sprinkled onto the external surface of the NWs, as would have been expected of SAAs**.**

The PtNi SAAs were used as electrocatalysts for HER, MOR, and EOR, wherein the performances of these SAA NWs consistently led to mass activities, which were all more than double that of pure Pt NWs alone. This observed increase in activity could be ascribed to the presence of not only a higher amount of active sites but also single atom Ni species. In the case of HER, the presence of Ni surface atoms which are bonded to two OH groups can modify the electronic properties of the surrounding Pt atoms, so as to decrease their hydrogen-binding

energy and correspondingly increase their activity. Similarly for the alcohol oxidation reactions, the presence of the Ni, decorating the external catalyst surface, can significantly diminish the possibility of deleterious CO adsorption as compared with bare Pt alone. In both cases, it is important to note that the single atom architecture itself is crucial in enabling the high performance, in that the presence of the Ni/Pt interface represents the driving force for improving electrocatalytic performance. Conversely, the incorporation of larger Ni clusters would ultimately lead to a decrease in activity, because the added Ni would likely cover a greater number of active Pt sites, thereby reducing the latter's catalytic participation. Overall, XAS offers a useful means with which to identify and confirm the local atomic and surface structure in order to improve the kinetics of different electrocatalytic reactions.[21]

Analogous **In-doped Pt ultrathin NWs** possessing sub-nanometer diameters were generated by a two-step solution based method in which (i) Pt NWs were initially formed followed by (ii) single atom doping with In. The doping process was accomplished by mixing in pre-made Pt NWs in oleylamine in the presence of $InBr_3$ as the In source. The atomic ratio of Pt / In was determined to be 95.2 / 4.8, using both ICP-AES and TEM-EDS methods. Moreover, HAADF-STEM images confirmed not only an ultrathin 1D morphology but also the formation of a single-atom architecture, wherein isolated In atoms were found to have dispersed across the external surfaces of the underlying Pt NWs.

These as-prepared wires were subsequently used as catalysts for HER and EOR.[22] In particular, the In-doped Pt NWs achieved a current density, which was ~4.1 times higher than that of Pt/C for HER under alkaline conditions. The Pt-In NWs also evinced better durability than Pt/C, by maintaining current densities of 10 mA cm^{-2} for at least 5 h, whereas the current densities for Pt/C control samples alone decreased sharply after just 1 h. In addition, the In-

doped Pt NWs yielded the highest measured activity for alkaline EOR, achieving a specific activity of 3.58 mA cm^{-2}, which was 1.9 and 2.1 times higher than that of Pt NWs and Pt/C, respectively. Moreover, under acidic conditions, the In-doped Pt NWs achieved a specific activity which was 2.5 times higher than that of Pt/C.

XAS data in this report were used to account for the local atomic and electronic structure of the wires. Specifically, the In *K*-edge XANES spectrum implied the formation of In_2O_3, whereas the complementary XANES and EXAFS spectra at the Pt L_3-edge were consistent with the presence of pure Pt. By analogy to what was observed with the PtNi SAAs, the EXAFS spectrum at the In *K*-edge only yielded a single peak, associated with the In-O bond, whereas there were no obvious peaks for either In-In or In-O-In bonds, intimating that In likely existed in the guise of isolated single atoms. The EXAFS and XANES spectra in Figure 2A-F are indicative of the In-O and In-Pt results. DFT calculations showed that the inclusion of single atoms of In can aid in reducing the limiting potential and thereby drive the release of H_2 in terms of promoting HER. In the context of EOR, the DFT calculations suggested that the In atoms facilitate the conversion of ethanol to acetate, as well as the desorption of the latter species less energetically demanding, thereby increasing the overall reaction's selectivity and activity.

In terms of different and perhaps more complex systems, Au-based core-shell ultrathin NWs, comprising **Au@Pd and Au@Ag_{ML}@Pd**, have been used as catalysts for EOR and 4-NP reduction.[13] The main benefit of a core-shell configuration in this case is that it can synergistically combine a catalytically active outer Pd shell with an inner AuPd core, conducive to increasing both measured activity and stability. The controlled growth of Ag and Pd monolayers (ML) was achieved by adding in successively smaller amounts of either silver nitrate or sodium tetrachloropalladate to a solution of pre-made Au ultrathin NWs. The resulting

Au@Ag$_{ML}$@Pd and Au@Pd architectures yielded superior catalytic EOR performance of 0.35 mA/μg and 0.51-0.64 mA/μg respectively, as compared with Pd wires and Pd/C commercial standards, which maintained comparatively poorer performance metrics. Furthermore, these Au@Ag$_{ML}$@Pd NW motifs were also reported to be ~100 fold more active for 4-NP reduction than other Au@Pd wires previously reported in the literature. To properly understand this degree of catalytic improvement, XAS measurements were collected to probe the wire structure. First, by comparing the Pd *K* edge white-line intensity, the order of signal reduction was observed to follow the trend of Pd NWs > Pd foil > Au@Pd NWs > Au@Ag$_{ML}$@Pd NWs. This finding was attributed to the comparative *d*-band filling of the Pd atoms within the Au@Ag$_{ML}$@Pd NWs as compared with either AuPd wires or pure Pd wires, and thought to account for the enhanced anti-oxidation capacity of Pd atoms in contact with either Au or Au/Ag.[13]

A 'first shell' EXAFS fitting was used to determine the coordination numbers of Pd, Au, and Ag atoms. Figure 2G shows FT-EXAFS of the Pd K edge associated with different Pd coverages, whereas Table 2 displays the complementary computed CN values. The EXAFS spectra revealed that in both Au@Pd and Au@Ag$_{ML}$@Pd, the Pd atoms are coordinated by either 5 to 7 Au or Ag atoms, which is higher than would otherwise have been expected for a Pd monolayer (i.e., 3 to 5). As such, it is apparent that some Pd atoms diffused into the sub-surface layer. The Au-Pd bond distance (2.82 Å) was consistent with the formation of an AuPd alloy, whereas the Pd-Pd bond distance (2.84 Å) elongated as compared with pure Pd nanowires alone (2.74 Å). This apparent increase in the Pd-Pd bond distance is likely due to increased surface strain, due to the formation of the Pd layer at the surface.

With the analogous Au@Pd samples, the CN for Pd-Pd was found to increase from 1.56 to 2.44, as the Pd layer grew in monolayer coverage. Specifically, whereas Au@Ag$_{ML}$@Pd

nanowires maintaining a Pd coverage of ½ ML possessed a Pd-Pd CN of 1.39, the sample incorporating a Pd coverage of 1/8 ML yielded Pd-Pd CN data less than 0.15. These low CN values revealed that the Pd atoms localized at the surface mostly existed as isolated Pd atoms. In terms of explaining the resulting catalytic enhancement, it was proposed that the geometry of Pd atoms, including bond lengths and surface strain, played a significant role in improving upon the EOR performance. Specifically, whether Pd was bound to either Au or Ag enabled different, distinctive synergistic effects of Au, such as either the removal of 'CO-like' intermediates or the promotion and exposure of reactive hydroxyl groups.[13]

***In situ* XAS on ultrathin nanowires**

In our group, *in situ* EXAFS was used to directly probe ultrathin PdAu@Pt NWs during the ORR reaction. In particular, these wires maintained a specific activity of ~1 mA/cm^2, about 5x higher than that of the Pt/C standard. With respect to their relevant synthesis, which is key to understanding their catalytic properties, the core PdAu NWs were initially generated using an air-sensitive room temperature solution-based method. To incorporate Pt as an outer shell on the surfaces of the inner underlying alloy, these as-synthesized NWs were successively subjected to a UV-ozone treatment, a CO stripping protocol, and finally an underpotential deposition (UPD) step. HAADF-STEM imaging, coupled with EELS line scans, implied the formation of NWs, wherein Pt and Au were both more concentrated at the surface, with Pd localized within the core. It is important to highlight that it is difficult to clearly differentiate Pt and Au atoms during the XAS fitting process, due to their similar photoelectron scattering properties. As such, the two elements were considered as equivalent entities during the fit.

Analysis of the corresponding Au L_3-edge EXAFS spectra yielded almost identical CN values of 6 for both the Au-Pd bond and the Au-Pt/Au bond, suggesting that Au exists either as

an interlayer between the Pd core and the Pt shell, or has been fully incorporated within the shell. This was an unexpected result, because the PdAu wires were previously assumed to comprise a homogeneous mixture. The only consistent picture that reconciled the collective Pt and Au results was one in which a uniform Pt-Au alloy was generated. Indeed, these EXAFS findings are consistent with the results obtained by an analogous EELS line scan, wherein Pt and Au atoms appeared to be spatially localized at the surface.[14]

It should be emphasized that these CNs were derived from data obtained after varying ORR cycle amounts from 0 to 1000. If there had been either degradation in the wires or an apparent change in the spatial positions of the elements during the reaction process itself, this would have been reflected in analogous alterations in the CNs, as calculated by the EXAFS fits; none of this occurred. Moreover, the corresponding CV curves taken throughout these runs also showed negligible differences. Hence, the reasoning behind the improvements in ORR stability was two-fold. First, the thin outer Pt shell reduced Pt oxidation as it was in contact with an underlying alloyed core substrate. Second, the Au sublayer led to a weaker absorption of oxygen, thereby inhibiting surface oxide formation and subsequently giving rise to higher stability within the reactive acidic media.[14]

In essence, EXAFS data not only deduced that the catalytically active structure of these ultrathin NWs consisted of a PtAu binary shell coupled with a pure inner Pd core but also rationalized the projected long-term stability of these samples.[14] It was in fact postulated that the plausible origin of the observed Au surface segregation might have been ascribed to the external potential used (i.e. 0.5-0.8 V) during the Cu UPD process used to create these hierarchically complex, ultrathin NWs in the first place.

Conclusions and Future Directions

As our Perspective has shown, there is a significantly greater body of *ex situ* (as compared with *in situ*) XAS data on ultrathin NWs. Hence, progress in this field will entail broader uses of *in situ* or *operando* XAS for additional and more generalized systems to obtain meaningful results during real-time catalytic measurements under realistic operating conditions. *In situ* XAS has already been performed on a wide variety of both metallic and oxide nanoparticles.[7-8] As such there is a significant amount of data that suggests that using *in situ* XAS techniques on ultrathin NWs is not only possible but necessary, as the trajectory of the field continues to develop. Indeed, *in situ* XAS data collected during catalytic reactions can address very specific, scientific questions. These include the following concerns.

(i) What localized structural alterations occur within the ultrathin NWs during the various electrochemical reaction processes and what are the causes of these changes?

(ii) What are the coordination modes of the reactive small molecules onto the surfaces of these wires? How does the bonding environment evolve?

(iii) What can XAS tell us about stability and degradation in real-time measurements?

Based on the *in situ* XAS data taken during the ORR reaction on PdAu@Pt core-shell NWs discussed earlier, it is evident that *in situ* XAS can be used to achieve insights into not only catalytic performance but also the long-term stability of ultrathin NW motifs.[14] To answer these questions more broadly, especially as a function of chemical composition, a wider variety of ultrathin NW electrocatalysts should be analyzed. Candidates include PtNi, PtRu, PtCo, and PtFe, which have shown promising performance metrics for ORR, EOR, and MOR.[23] As evidence for the value of this type of effort, carbon dioxide electroreduction (CO_2RR), the

oxygen evolution reaction (OER), and ORR have already been widely studied using *in situ* XAS in the context of other types of nanomaterial motifs and nanoscale morphologies.[7-8]

Nevertheless, daunting challenges remain. As a pervasive concern, XAS techniques tend to require the production of high-quality samples in reasonably large quantities, which is a non-trivial task in the case of ultrathin NWs. Moreover, *ex situ* XAS analysis is difficult in samples characterized by either (i) a mixture of morphologies, (ii) compositional polydispersity, or (iii) the presence of dilute elements. By comparison, the use of *in situ* techniques can be limited by these identical issues as well as additional complications arising from (a) the non-uniform deposition of catalysts on the working electrode, (b) the presence of reaction media containing inhomogeneities in reagent chemical compositions, (c) poor detection limits emanating from either low concentrations of reactants or electrolytes, (d) harsh reaction conditions, and/or (e) the presence of a multitude of different chemical structures that may give rise to dissimilar active sites and observed reactivity in the reaction process.

In addition, there are a myriad of technical issues that cannot be ignored. *First*, the liquid cell chamber used for experimentation must not only be compatible with extant beam-line conditions but also the electrochemical reaction medium, because the cell configuration incorporating the working electrode, coated with the sample in question, is placed directly in the pathway of the incoming X-ray beam.[8] As examples, customized cells have been created for the *in situ* study of growing Pd/Pt bimetallic nanoclusters[17] and Au-Pt nanoparticles.[24] It is not altogether evident that these will also work for ultrathin NWs.

Second, the timing of the reaction process is a key consideration; some electrocatalytic reactions occur over the course of seconds (or even shorter time frames) whereas others may transpire over hours and days. Enabling time-resolved XAS (TR-XAS) entails achieving

appropriate time resolution, while simultaneously ensuring that data quality is maintained. As an example, TR-XAS allows for structural data to be acquired on a $(Ru(bpy)_2(py)_2)^{2+}$ system with a time resolution as low as 100 ps, but the setup is complex and involves the use of a specialized pump/probe set up that is not widely available.[25]

Third, XAS represents a 'bulk averaged' technique, and is limited in its ability to analyze the nature of activities occurring on the external surfaces of as-generated samples. In particular, because hard XAS involves energies over 5 keV with a high penetration depth, the technique has a limited sensitivity with respect to probing localized and nuanced phenomena occurring on the outer surfaces of materials.[7] In principle, due to their very small size, it is worth mentioning that ultrathin NWs possess a proportionately larger number of surface atoms versus their bulk, such that any electrochemical activity detected will necessarily be dominated by surface interactions.[7] A useful detection strategy would be to analyze trends associated with the electron yield of electrons characterized by relatively short mean free paths (1-5 nm); however, the problem is that this data collection mode tends to operate successfully under vacuum conditions, as opposed to the potentially corrosive liquid-based environments typical of electrocatalysis.[7-8]

Given all of the limitations, it is reasonable to assert that only a combined and collective consideration of the results generated by not only XAS but also many other complementary characterization techniques described earlier will enable an accurate and holistic representation of the local atomic and electronic structure of ultrathin NW motifs. Moreover, the products of these diverse experimental efforts would be inherently strengthened and rationalized by theoretical studies that could assist in addressing lingering questions about the evolving real-time dynamic behavior of actual electrocatalysts operating under realistic conditions, relevant to commercial applications.

Acknowledgements

This material is based on work performed in SSW's laboratory, supported by the U.S. National Science Foundation under Grant No. CHE-1807640. N. H. acknowledges financial support from a Joint Photon Sciences Institute (JPSI) graduate student fellowship for work derived from experiments performed at Brookhaven National Laboratory.

References

1. Xia, Y.; Yang, P.; Sun, Y.; Wu, Y.; Mayers, B.; Gates, B.; Yin, Y.; Kim, F.; Yan, H., One-Dimensional Nanostructures: Synthesis, Characterization, and Applications. *Adv. Mater.* **2003,** *15*, 353-389.
2. Cademartiri, L.; Ozin, G. A., Ultrathin Nanowires: A Materials Chemistry Perspective. *Adv. Mater.* **2009,** *21* (9), 1013-1020.
3. Frenkel, A., Applications of Extended X-ray Absorption Fine-Structure Spectroscopy to Studies of Bimetallic Nanoparticle Catalysts. *Chem. Soc. Rev.* **2012,** *41* (24), 8163-8178.
4. Gurman, S. J., Interpretation of EXAFS Data. *J. Synchrotron Radiat.* **1995,** *2*.
5. Rehr, J. J.; Albers, R. C., Theoretical Approaches to X-ray Absorption Fine Structure. *Rev. Mod. Phys.* **2000,** *72* (2), 621-654.
6. Natoli, C. R.; Benfatto, M.; Della Longa, S.; Hatada, K., X-ray Adsorption Spectroscopy: State-of-the-art Analysis *J. Synchrotron Radiat.* **2003,** *10*, 26-42.
7. Wang, M.; Arnadottir, L.; Xu, Z. J.; Feng, Z., In Situ X-ray Absorption Spectroscopy Studies of Nanoscale Electrocatalysts. *Nanomicro Lett.* **2019,** *11* (1), 47 (1-18).
8. Timoshenko, J.; Roldan Cuenya, B., In Situ/Operando Electrocatalyst Characterization by X-ray Absorption Spectroscopy. *Chem. Rev.* **2021,** *121* (2), 882-961.
9. Pschunder, F.; Puig, J.; Giovanetti, L. J.; Huck-Iriart, C.; Requejo, F. G.; Buceta, D.; Hoppe, C. E.; Ramallo-López, J. M., New Insights into the Growth Mechanism of Ultrathin Au Nanowires from Combined in Situ EXAFS and SAXS Studies. *J. Phys. Chem. C* **2018,** *122* (50), 29051-29061.
10. McGuire, S. C.; Ebrahim, A. M.; Hurley, N.; Zhang, L.; Frenkel, A. I.; Wong, S. S., Reconciling Structure Prediction of Alloyed, Ultrathin Nanowires with Spectroscopy. *Chem. Sci.* **2021,** *12* (20), 7158-7173.
11. Kunze, S.; Grosse, P.; Bernal Lopez, M.; Sinev, I.; Zegkinoglou, I.; Mistry, H.; Timoshenko, J.; Hu, M. Y.; Zhao, J.; Alp, E. E.; Chee, S. W.; Roldan Cuenya, B., Operando NRIXS and XAFS Investigation of Segregation Phenomena in Fe-Cu and Fe-Ag Nanoparticle Catalysts during CO_2 Electroreduction. *Angew. Chem. Int. Ed. Engl.* **2020,** *59* (50), 22667-22674.
12. Ge, J.; He, D.; Chen, W.; Ju, H.; Zhang, H.; Chao, T.; Wang, X.; You, R.; Lin, Y.; Wang, Y.; Zhu, J.; Li, H.; Xiao, B.; Huang, W.; Wu, Y.; Hong, X.; Li, Y., Atomically Dispersed Ru on Ultrathin Pd Nanoribbons. *J. Am. Chem. Soc.* **2016,** *138* (42), 13850-13853.
13. Liu, R.; Zhang, L. Q.; Yu, C.; Sun, M. T.; Liu, J. F.; Jiang, G. B., Atomic-Level-Designed Catalytically Active Palladium Atoms on Ultrathin Gold Nanowires. *Adv. Mater.* **2017,** *29* (7), 1604571 (1-8).
14. Liu, H.; An, W.; Li, Y.; Frenkel, A. I.; Sasaki, K.; Koenigsmann, C.; Su, D.; Anderson, R. M.; Crooks, R. M.; Adzic, R. R.; Liu, P.; Wong, S. S., In Situ Probing of the Active Site Geometry of Ultrathin Nanowires for the Oxygen Reduction Reaction. *J. Am. Chem. Soc.* **2015,** *137* (39), 12597-12609.
15. Chen, Z.; Higgins, D.; Yu, A.; Zhang, L.; Zhang, J., A Review on Non-Precious Metal Electrocatalysts for PEM Fuel Cells. *Energy Environ. Sci.* **2011,** *4*, 3167-3192.
16. Morozan, A.; Jousselme, B.; Palacin, S., Low-Platinum and Platinum-Free Catalysts for the Oxygen Reduction Reaction at Fuel Cell Cathodes. *Energy Environ. Sci.* **2011,** *4* (4), 1238-1254.

17. Chen, C.-H.; Hwang, B.-J.; Wang, G.-R.; Sarma, L. S.; Tang, M.-T.; Liu, D.-G.; Lee, J.-F., Nucleation and Growth Mechanism of Pd-Pt Bimetallic Clusters in Sodium Bis(2-ethylhexyl)sulfosuccinate (AOT) Reverse Micelles as Studied by in Situ X-ray Absorption Spectroscopy. *J. Phys. Chem. B* **2005,** *109*, 21566-21575.
18. Li, M.; Zhao, Z.; Cheng, T.; Fortunelli, A.; Chen, C.-Y.; Yu, R.; Zhang, Q.; Gu, L.; Merinov, B. V.; Lin, Z.; Zhu, E.; Yu, T.; Jia, Q.; Guo, J.; Zhang, L.; Goddard, W. A.; Huang, Y.; Duan, X., Ultrafine Jagged Platinum Nanowires Enable Ultrahigh Mass Activity for the Oxygen Reduction Reaction. *Science* **2016,** *354*, 1414-1419.
19. Kong, F.; Banis, M. N.; Du, L.; Zhang, L.; Zhang, L.; Li, J.; Doyle-Davis, K.; Liang, J.; Liu, Q.; Yang, X.; Li, R.; Du, C.; Yin, G.; Sun, X., Highly Stable One-Dimensional Pt Nanowires with Modulated Structural Disorder Towards the Oxygen Reduction Reaction. *J. Mat. Chem. A* **2019,** *7* (43), 24830-24836.
20. Huang, H.; Li, K.; Chen, Z.; Luo, L.; Gu, Y.; Zhang, D.; Ma, C.; Si, R.; Yang, J.; Peng, Z.; Zeng, J., Achieving Remarkable Activity and Durability Toward Oxygen Reduction Reaction Based on Ultrathin Rh-Doped Pt Nanowires. *J. Am. Chem. Soc.* **2017,** *139* (24), 8152-8159.
21. Li, M.; Duanmu, K.; Wan, C.; Cheng, T.; Zhang, L.; Dai, S.; Chen, W.; Zhao, Z.; Li, P.; Fei, H.; Zhu, Y.; Yu, R.; Luo, J.; Zang, K.; Lin, Z.; Ding, M.; Huang, J.; Sun, H.; Guo, J.; Pan, X.; Goddard, W. A.; Sautet, P.; Huang, Y.; Duan, X., Single-Atom Tailoring of Platinum Nanocatalysts for High-Performance Multifunctional Electrocatalysis. *Nat. Catal.* **2019,** *2* (6), 495-503.
22. Zhu, Y.; Zhu, X.; Bu, L.; Shao, Q.; Li, Y.; Hu, Z.; Chen, C. T.; Pao, C. W.; Yang, S.; Huang, X., Single-Atom In-Doped Subnanometer Pt Nanowires for Simultaneous Hydrogen Generation and Biomass Upgrading. *Adv. Funct. Mater.* **2020,** *30* (49), 2004310 (1-11).
23. Wang, Y.; Yuan, Y.; Huang, H., Recent Advances in Pt-Based Ultrathin Nanowires: Synthesis and Electrocatalytic Applications. *Chin. J. Chem.* **2021,** *39* (5), 1389-1396.
24. Nayak, C.; Bhattacharyya, D.; Bhattacharyya, K.; Tripathi, A.; Bapat, R.; Jha, S.; Sahoo, N., Insight into Growth of Au-Pt Bimetallic Nanoparticles: an In-Situ XAS Study. *J. Synchrotron Radiat.* **2017,** *24* (Pt 4), 825-835.
25. Borfecchia, E.; Garino, C.; Gianolio, D.; Salassa, L.; Gobetto, R.; Lamberti, C., Monitoring Excited State Dynamics in cis-$[Ru(bpy)_2(py)_2]^{2+}$ by Ultrafast Synchrotron Techniques. *Catalysis Today* **2014,** *229*, 34-45.

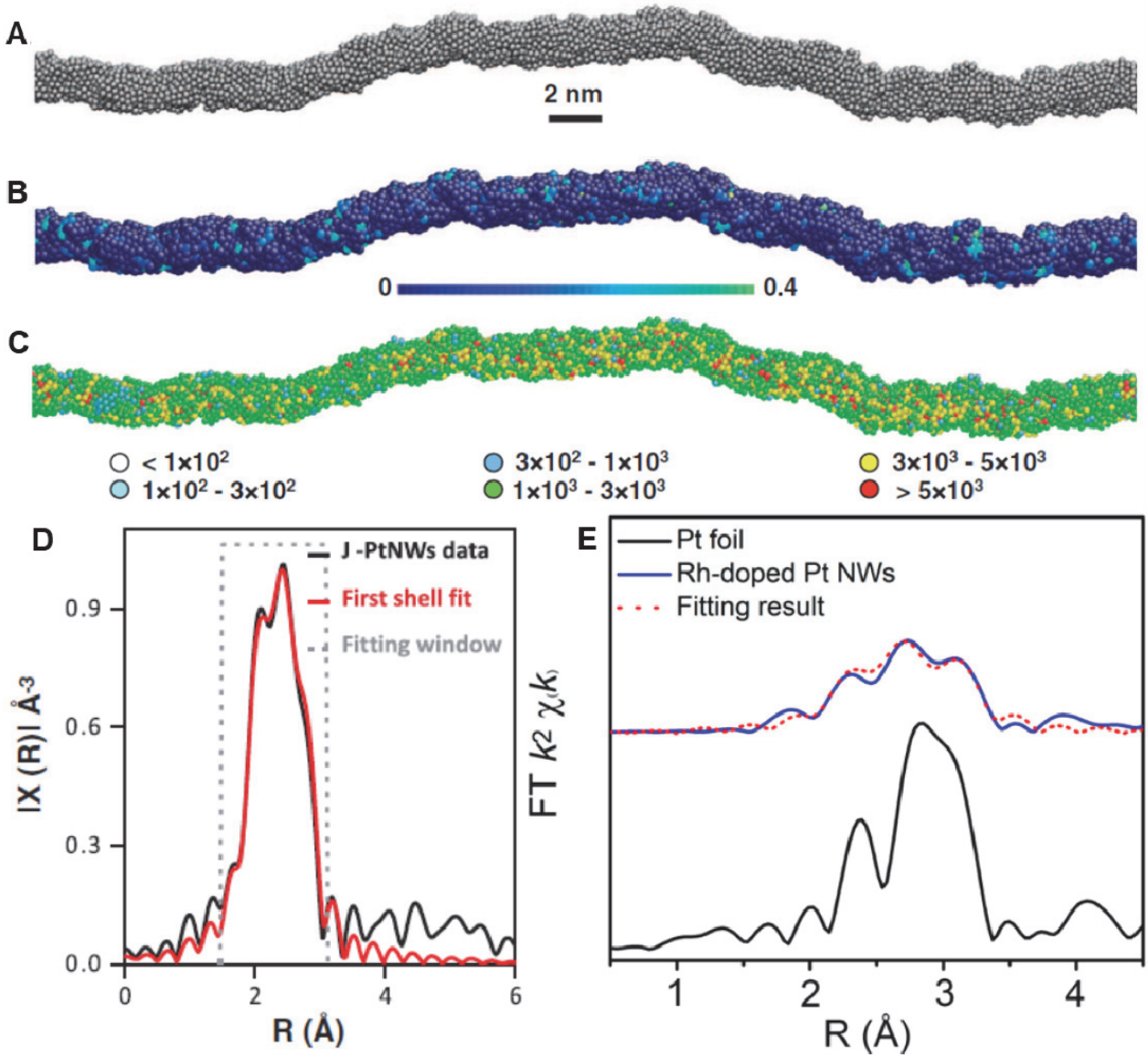

Figure 1. (A) Schematic of the J-Pt NW generated by simulations. **(B)** The five-fold index of the J-Pt NW shown with colored atoms. **(C)** J-Pt NW schematic indicates the distribution of atomic stress (in atm·nm^{-3}). **(D)** Pt L3 edge FT-EXAFS spectrum (black) was collected ex situ with the corresponding first-shell fit (red) for the J-Pt NWs. Reprinted with permission from reference 18. Copyright 2016 The American Association for the Advancement of Science. **(E)** Pt L3-edge EXAFS spectra (blue) is shown in R space for Rh-doped Pt NWs with the corresponding fitted curve (red) and the Pt foil reference (black). Reprinted with permission from reference 20. Copyright 2017 American Chemical Society.

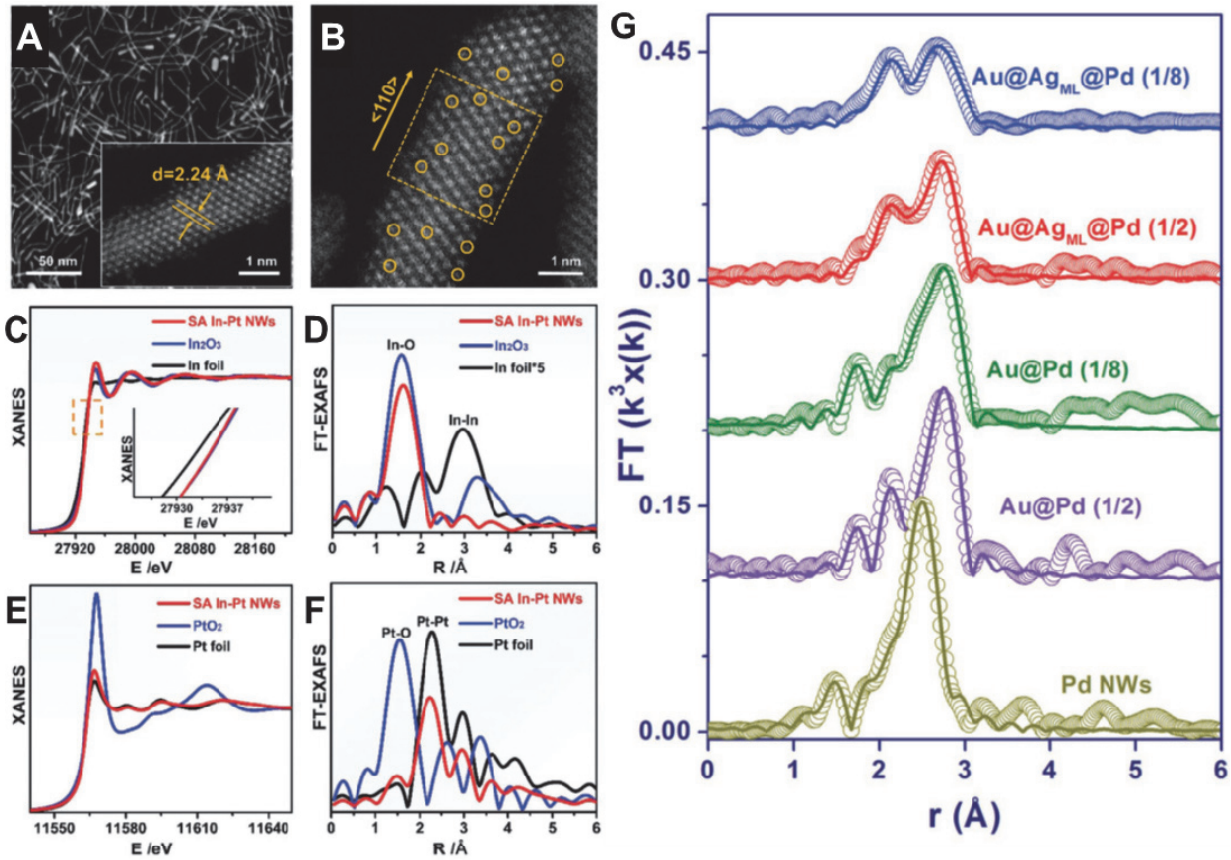

Figure 2. (A) HAADF-STEM images of the In-Pt NWs and **(B)** high resolution aberration corrected HAADF-STEM images with the individual In atoms highlighted. **(C)** XANES spectrum and **(D)** Fourier transform EXAFS of the In K-edge for the SA In-Pt NWs, In foil, and In_2O_3, respectively. **(E)** XANES spectrum for the Pt L3-edge and **(F)** Fourier transformed EXAFS of the Pt L3-edge for SA In-Pt NWs, Pt foil, and PtO_2, respectively. Reprinted with permission from reference 22. Copyright 2020 John Wiley and Sons. **(G)** The Fourier transformed EXAFS Pd K-edge spectra for different amounts of of Pd and Ag/Pd on the Au NWs. Reprinted with permission from reference 13. Copyright 2016 John Wiley and Sons.

Material System	Nature of the Bond	Coordination number	Bond distance (Å)	Reference
J-Pt NWs	Pt-Pt	6-8	2.71	[18]
Pt foil	Pt-Pt	12	2.76	
D-O_2-Pt NWs	Pt-Pt	7.59	N/A	[19]
D-O_2-Pt NWs	Pt-O	0.5	N/A	
Pt/C	Pt-Pt	9	N/A	
PtRh	Pt-Pt	8.0	2.74	[20]
PtRh	Pt-Rh	1.2	2.69	

Table 1. Coordination numbers and bond distances of the relevant NWs, described in the ex situ analysis of ultrathin monometallic and alloy-based nanowires.

Material System	Nature of the Bond	Coordination number	Bond distance (Å)	Reference
SAAs of Ni-Pt NWs	Pt-Pt	8.9	2.74	[21]
SAAs of Ni-Pt NWs	Ni-O	2.3	2.04	
Pd foil	Pd-Pd	12	2.71	[13]
Pd NWs	Pd-Pd	7.28	2.74	
	Pd-O	1.05	1.99	
Au@Pd (1/2) NWs	Pd-Au	6.11	2.84	
	Pd-Pd	2.44	2.88	
Au@Pd (1/8) NWs	Pd-Au	5.57	2.86	
	Pd-Pd	1.33	2.84	
Au@Ag_{ML}@Pd (1/2) NWs	Pd-Ag	4.51	2.83	
	Pd-Au	1.87	2.84	
	Pd-Pd	1.25	1.99	
Au@Ag_{ML}@Pd (1/8) NWs	Pd-Ag	4.21	2.81	
	Au-Pd	2.37	2.83	
	Pd-Pd	N/A	N/A	

Table 2. Coordination numbers and bond distances of the relevant NWs, discussed in the ex situ analysis of ultrathin single-atom and core-shell nanowires.

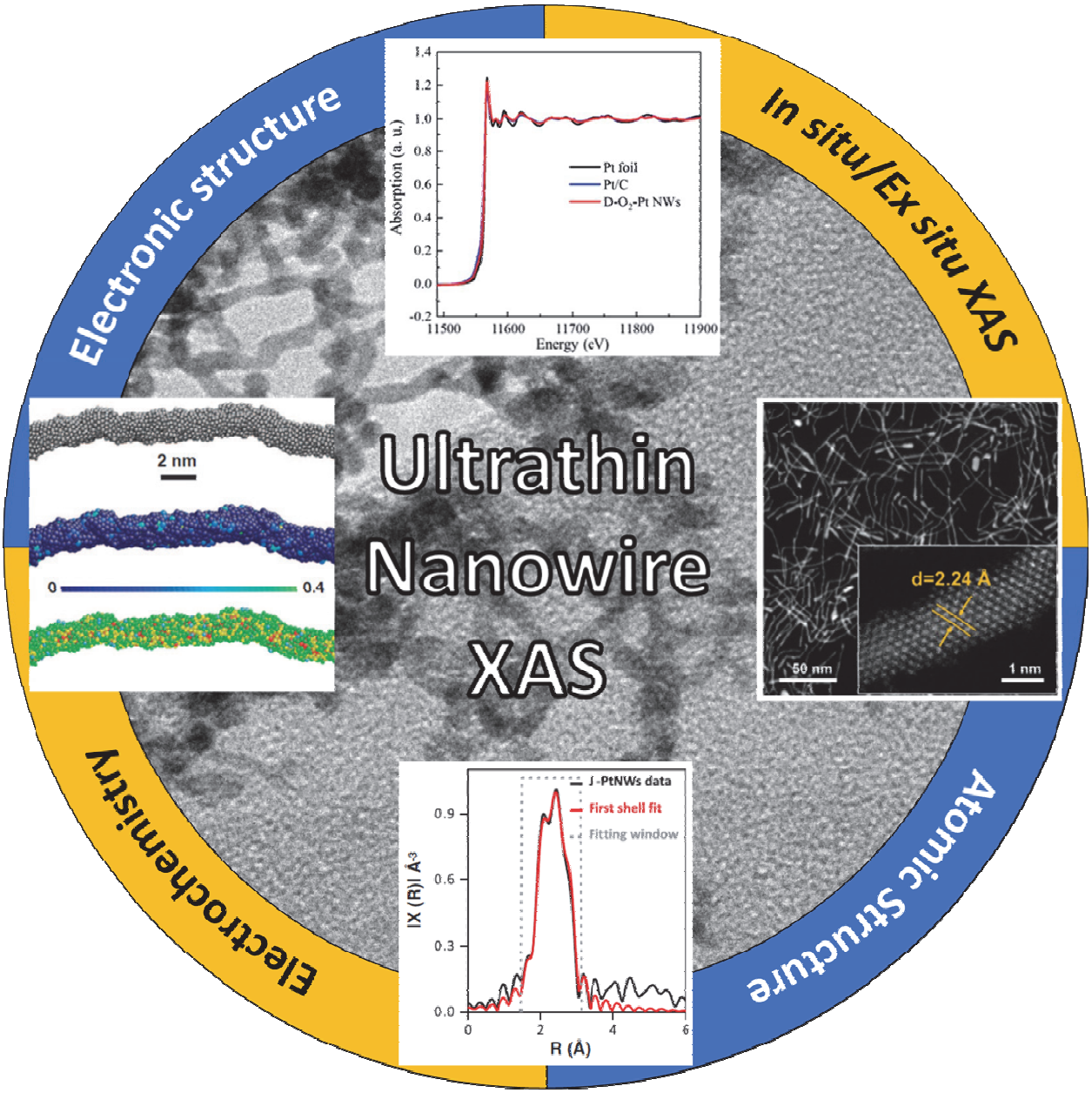

Table of Contents Figure